

**Military Technical College  
Kobry El-Kobbah,  
Cairo, Egypt**



**6<sup>th</sup> International Conference  
on Electrical Engineering  
ICEENG 2008**

## **Thermal modeling of a high fill-factor micromachined bolometer for thermal imaging applications**

*By*

M.Safy \*

A.Hafz Zaky \*

A.Mitkes \*

### **Abstract:**

Infrared radiation bolometer which is made of thin film of a Si:H is thermally modeled using 3-d finite element analysis method (FEA). This bolometer is realized in a multilevel electro thermal structure having high fill factor. Using the multilevel structure, thermal isolation can be independently optimized without sacrificing IR absorption area. The design shows that thermal time constant of 12.95 ms, responsivity of  $4.65 \times 10^3 \text{ V/W}$ , and detectivity of  $7.97 \times 10^8 \text{ cm Hz}^{1/2} \text{ W}^{-1}$  can be achieved in  $50 \mu\text{m} \times 50 \mu\text{m}$  micromachined structure.

### **Keywords:**

Bolometer-Infrared- Thermal Modeling-Micromachined-Detectors-FEA

---

\* Egyptian Armed Forces

## 1. Introduction:

Merging the micromachined techniques with thermal bolometers has led to the ability of fabrication of uncooled devices having comparable performance to its cooled photonic counterparts, this also provided the ability of integration of array readout circuits with bolometer arrays using the same IC processing techniques hence lowering the cooling cost, overall fabrication cost.

Surface micromachined uncooled detectors are mostly based on microbolometer approach, where infrared radiation heats the sensor material through an absorbing mechanism, changing its resistance according to its temperature coefficient of resistance (TCR) of its active material. This approach allows the implementation of small pixel sizes, such as  $50\mu\text{m} \times 50\mu\text{m}$ . Vanadium oxide ( $\text{VO}_x$ ), the most widely used material has a TCR of about 2-3% /K [1], however  $\text{VO}_x$  is not a standard material in IC fabrication. Other materials such as amorphous silicon [2] and poly silicon SiGe [3] have also high TCR values of 3-6%/k and 2-3%, respectively. However these materials requires high temperature annealing. We believe that greater design flexibility is provided using amorphous silicon semiconductors [4,5,6] as will discussed later.

The fill factor is the detection area to the detector area; its values depend on the structure and the shape of the supporting leg. The metal bolometer is realized in a multilevel electro thermal structure with a fill factor over 92% [7], and for amorphous silicon values of 51% and 80% could be achieved [6, 8]. The objective of this paper to make a model of the mostly used bolometers, then optimizing the bolometer from compatibility, design flexibility, TCR, fill factor and thermal isolation points of view.

## 2. Modeling of common used bolometer Structures:

The bolometers under study are metal active material and semiconductor supporting leg [9] as shown in figure.1, the other Bolometer with semiconductor active material and metal supporting leg [10] as shown in figure.2. The first case, [9] the microbolometer element has an area of  $50 \times 50 \mu\text{m}$  and approximately  $1 \mu\text{m}$  thick. It consists of a layer of vanadium oxide ( $\text{VO}_2$ ) sandwiched between two layers of silicon nitride ( $\text{Si}_3\text{N}_4$ ).  $\text{VO}_2$  is used as active material because of its reasonable TCR. Under these layers a  $\lambda/4$  air absorber with height  $2.5 \mu\text{m}$  for maximum absorption at  $10 \mu\text{m}$  is constructed.

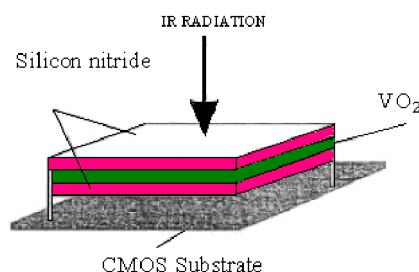


Figure.1 Schematic drawing of Vanadium oxide microbolometer.

The second case [10] the microbolometer element has an area of  $40\mu\text{m}\times 40\mu\text{m}$ . It consists of 3-layers of Ni-Cr, aSi:H and Ti metal support at each corner is defined by length= $10\mu\text{m}$ , width= $5\mu\text{m}$  and a thickness = $0.1\mu\text{m}$ . The supports are comprised of nichrome alloy. Which has a thermal conductivity of  $0.12\text{ w.cm}^{-1}.\text{K}^{-1}$

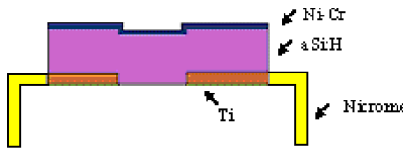


Figure.2 Schematic drawing of Semiconductor microbolometr.

In the following thermal modeling of these two structures will be done compared to published data *Thermal analysis of the bolometers*

In this work the heat transfer within the detector has been solved by using the computational fluid dynamics (CFD) model. This model has been solved to predict the behavior of the heat to the resistive material. CFD program has been used to solve the heat transfer through the detector.

In order to determine the heat transfer behavior, the following procedure must be carried out

#### *Geometry setup and grid generation*

First step of CFD model is the description and definition of the domain where the heat will pass through, known as preprocessing of model. The preprocessing procedures include geometry setup of the domain, meshing the domain and definition the boundary conditions.

The detectors main dimensions are:

#### 1-VO<sub>2</sub> microbolometer

A layer of vanadium oxide (VO<sub>2</sub>) having dimensions of  $50\times 50\times 0.1\mu\text{m}$

Two layers of silicon nitride (Si<sub>3</sub>N<sub>4</sub>)  $50\times 50\times 0.45\mu\text{m}$  each

The supporting leg consists of Si<sub>3</sub>N<sub>4</sub> and titanium of  $2.5\times 5\times 3\mu\text{m}$  each

#### 2-Amorphous silicon microbolometer

Nickel Chromium layer of  $50\times 50\times 0.01\mu\text{m}$

Amorphous silicon resistive layer of  $50\times 50\times 0.8\mu\text{m}$

Reflective Titanium layer of  $50\times 50\times 0.1\mu\text{m}$

Supporting with nichrome alloy of  $10\times 5\times 0.1\mu\text{m}$

The total numbers of mesh element of detectors are 398572 elements for amorphous silicon microbolometer and 248532 for VO<sub>2</sub>

**Boundary conditions definitions**

Boundary conditions specify the flow and thermal variables on the boundaries of the CFD model.

They are, therefore a critical component of the CFD simulations and it is important that they are specified appropriately. In CFD, boundary conditions are associated with zones, not with individual faces or cells.

In this case the boundary conditions have been defined by three types of thermal conditions:

1-Fixed heat flux

The bolometers exposed to constant heat flux of 0.1 μw for VO2 bolometer and 3.88μW for amorphous silicon bolometer.

2-Conduction

The bolometer consists of stacked layers, so the incident heat radiate from layer to another by radiation

3- Radiation

Bolometers are operated in vacuum conditions so transfer of heat by radiation only

**Results**

FEA calculations were performed for the two design variants. Temperature distribution for both structures is shown in figure3,4 respectively. Temperature variants can be extracted from these figures.

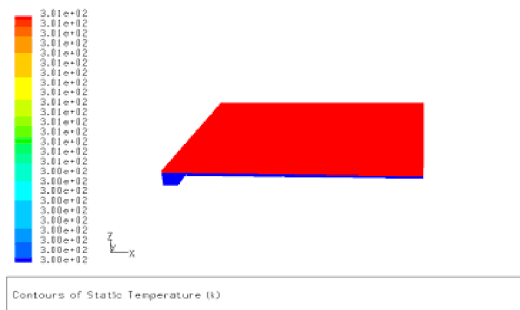


Figure.3 3-D temperature distribution of VO<sub>2</sub> microbolometer

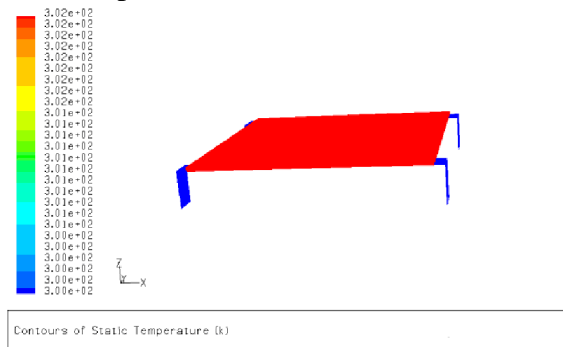


Figure.4 3-D temperature distribution of amorphous silicon microbolometer

Table.1 Comparison between simulation result and published result for temperature variants.

	Published results	Simulation results
vanadium oxide bolometer	NA	3k
amorphous silicon bolometer	1.98K	2k

The table shows that higher temperature variants between the bolometer and the ambient could be achieved for semiconductor bolometer due to the fact that it is supported by its thin metal legs ( $0.1\mu\text{m}$ ) compared to the thick ( $0.3\mu\text{m}$ ) semiconductor legs of the  $\text{VO}_x$  bolometer.

**3. Proposed optimum structure:**

Upon comparing the two structures we find that, although the first structure has a high fill factor, however it suffers some disadvantages. The absorber underneath it requires hard fabrication constrains for maintaining uniform  $2.5\mu\text{m}$  height in the presence of layer stress that can cause structure buckling downwards or upwards. This also constrains the thermal isolation mechanism. Taking into consideration that  $\text{VO}_x$  is not a standard IC material, we can conclude that semiconductor bolometer is much promising for optimizing.

Semiconductor bolometer is better for the following reasons, the absorber is formed by the bolometer it self, so no restrictions on the fabrication associated with  $2.5\mu\text{m}$ .

Higher thermal insulation can be achieved as discussed before. Thermal isolation and fill factor can be optimized separately.

The proposed bolometer structure is a sandwich-gap consists of two sandwich elements in series, with a gap component in parallel [11].

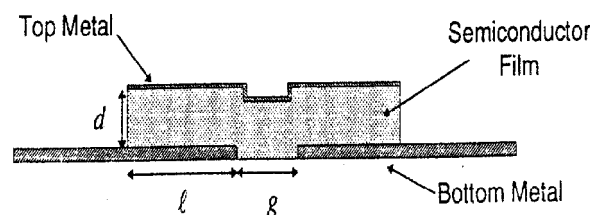


Figure .5 Sandwich –Gap geometry

For achieving high thermal isolation and high fill factor, this bolometer is to realized in a electrothermal structures [7].

The proposed structure is shown in Figure.6. The bottom metal consists of a thermally evaporated 10 ohm/sq titanium reflector, a quarter-wave length absorber which consists of active material for the bolometer and nickel chromium film which is impedance matched to free space having a resistivity of 377 ohm/sq.

Titanium was chosen for the reflector film because it gives excellent adhesion, has low film stress and good mechanical properties. Note that the bottom metal also supplies the electrical connection to the bolometer and provides the mechanical support for the thermal isolation structure. This type of detector has the potential of yielding 90% absorption integrated over the 8-14 $\mu$ .m wave band [10].

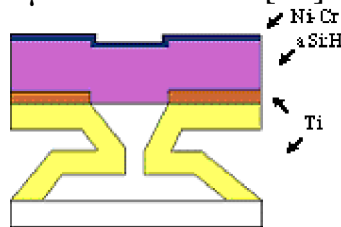


Figure.6 Proposed high fill-factor bolometer using surface micromachined multilevel structure

a.Si:H was chosen because by optimizing deposition parameters of hydrogenate amorphous silicon (a.Si:H) thin film, superior thermistors with a high temperature coefficient of resistance and low electronic excess noise will be obtained [8]. The a.Si:H is then covered by thin Ni-Cr top metal layer

The 377 ohm/sq metal absorber layer is impedance matched to free space: hence 50% of the incident radiation is absorbed and 50% transmitted, with none reflected. The transmitted portion of the radiation travels through the quarter-wave semiconductor layer, is reflected by the lower metal film, and destructively interferes with the incident wave, giving zero reflection and almost 100% absorption.

The bottom part of Figure.6 shows the multilevel electro thermal isolation structure of the proposed bolometer. The first level forms the suspended arms which are mechanically supporting the top IR absorbing area by connecting it to substrate. High fill factor, high thermal isolation can be achieved from optimizing the dimension and layout of the arms due to folding underneath the bolometer.

### 3.1 Predicted performance

Prediction for the performance in vacuum is obtained using both simple analytical expressions for thermal conductance, time rise and time constant

Parameters used for performance calculation are contained in table.2

Table.2 Definition of parameters associated with microbolometer

Symbol	Description
$\rho$ (aSi:H)	The resistivity =430.33 $\Omega$ .m
$g$	The gap length=6 $\mu$ .m
$d$	The thickness=0.8 $\mu$ .m
$w$	The detector side length=50 $\mu$ .m
$l$	The length of the bottom layer=22 $\mu$ .m
$K$	The thermal conductivity of the thermal path=7.44 w. (m.K) <sup>-1</sup>
$A_p$	The crosssectional area of the thermal path=5X0.3X10 <sup>-12</sup> m <sup>2</sup>
$L$	the length of the thermal path=50 $\mu$ m
$I$	The bias current=2 $\mu$ A
$R$	The detector resistance=6.19X10 <sup>5</sup> $\Omega$
$\alpha$	TCR=0.022/K <sup>0</sup>
$\zeta$	The emissivity=1
$G$	The thermal conductivity=4.45X10 <sup>-7</sup> W/KK
$B$	The bridge factor= (R <sub>L</sub> / (R <sub>L</sub> +R))=0.5
$R_L$	Load resistance=R
$A$	The detector area [w(2d <sup>2</sup> +l <sub>2</sub> g)]
$V_n$	The total detector noise=2.9X10 <sup>-8</sup> v/Hz <sup>1/2</sup> At 80 Hz
$C$	The total thermal capacitance=5.79 J/K

The detector resistance is given by:

$$R = \rho \frac{2dg}{w(2d^2 + l_2g)} = 6.19 \times 10^5 \Omega$$

The thermal conductance is given by:

$$G = K (A_p/L) = 4.45 \times 10^{-7} \text{W/K}$$

The responsivity is given by:

$$R_V = \frac{BIR\alpha}{G(1+4\pi^2 f^2 \tau^2)^{1/2}} = 4.65 \times 10^3 \text{V/W at 80 Hz}$$

The detectivity is given by:

$$D^* = \frac{R_V \sqrt{A}}{V_n} = 7.97 \times 10^8 \text{cmHz}^{1/2} \text{w}^{-1}$$

The thermal time constant:

$$\tau = \frac{C}{G} = 12.95 \text{m sec}$$

Table.3 Properties bolometer materials

	Thermal conductivity (w/mk)	Specific Heat (J/Kg.K)	Density (Kg/m <sup>3</sup> )
Ni-Cr	5	388.23	8500
aSi:H	9	1000	2350
Ti	7.44	544.25	4850

**3.2 Thermal modeling:**

Same procedure were carried out of thermal modeling of the proposed structure,3-D temperature distribution is shown in figure.7

From the 3-D finite element analysis variant temperature through the detector is extracted, having a value of  $\Delta T=8.4K$

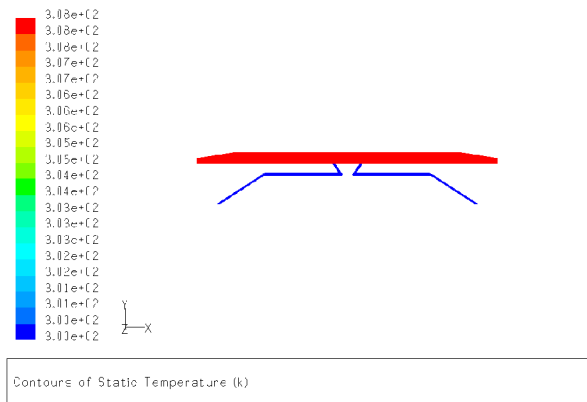


Figure.7 3-D temperature distribution of the proposed structure

**4 Conclusion:**

An optimized structure for a semiconducting micromachined microbolometer was introduced. Its predicted performance had values of  $\tau=12.5$  ms,  $R_v= 4.65 \times 10^3$  V/W, and  $D^* = 7.97 \times 10^8$  cm Hz<sup>1/2</sup>w<sup>-1</sup> which has a high fill factor over 92%.This structure provides a great flexibility for fabrication processed, enables independent optimization of the thermal conductance. The structure was 3-D modeled, temperature variant was found to be 8.4 K. We believe that using a higher TCR amorphous silicon materials having well defined noise will further increase the bolometer performance .

**References:**

- [1] R.A.Wood, "Uncooled Thermal Imaging Monolithic Silicon Focal Arrays," *Infrared Technology XIX Proc.SPIE*, 2020, 322 (1993).
- [2] Tsutomu Ichihara, Yoshifumi Watabe, Yoshiaki Honda and Kouichi Aizawa, "A High Performance Amorphous Si<sub>1-x</sub>C<sub>x</sub>: H Thermistor Bolometer Based on Micro-Machined Structure," *International conference on solid state sensors and Actuators*, Chicago, June 1997.
- [3] S.Sedky, Paolo Fiorini, Matty Caymax, Agnes Verbist, Chris Bart, "IR bolometer made of polycrystalline silicon germanium," *Sensor and actuators A66* (1998) 193-199.
- [4] J.Brady , T.Schimert , D.Ratcliff , R.Gooch, B .Richet, P.McCardel ,K.Rachel, "Advanced in amorphous silicon uncooled IR systems," *SPIE Vol.3698*, April 1999.
- [5] K.C. Liddiard, M.H.Unewisse and O.Reinhold, "Design and fabrication of thin film monolithic uncooled infrared detector arrays," *SPIE Vol,2225*.1994.
- [6] I.F. Brady, "Advanced in amorphous silicon uncooled IR systems," *Proc. SPIE Vol. 3698, Infrared Technology and Applications XXV*, p; 161 (1999).
- [7] Hyung-Kew Lee, Jun-Bo Yoon, Euisik Yoon, Sang-Baek ju, Yoon-Joong Yong, Wook Lee, and Sang-Gook Kim, "A high fill factor infrared bolometer using micromachined multilevel electrothermal structures," *IEEE Transactions on electron devices*, vol.46. No.7, July 1999.
- [8] J-L Tissot et al., "LETI/LIR's amorphous silicon uncooled microbolometer development," *Proc. SPIE Vol. 3379, Infrared Detectors and Focal Plane Arrays* 111(1994).
- [9] Paul J. Thomas, Alexander Savchenko, Peter Sinclair , Paule Goldman , Richard Hornsby , Canaan Hong , Timothy Pope , "Offset and gain compensation in an integrated bolometer array ," *SPIE ,Vol.3698*, April 1999.
- [10] M.H.Unewisse, S.J.Passmore, K.C.Liddiard and R.J.Watson "Performance Of Uncooled Semiconductor Film Bolometer Infrared Detector", *SPIE Vol.2269 Infrared technology XX* (1999).
- [11] K.C.Liddiard, M.H.Unewisse and O.Reinhold, "Design and fabrication of thin film monolithic uncooled infrared detector arrays," *SPIE Vol,2225*.1994.